

## The fate of cerium oxide nanoparticles in sediments and their routes of uptake in a freshwater worm

Richard K. Cross<sup>a,b</sup> , Charles R. Tyler<sup>a</sup> and Tamara S. Galloway<sup>a</sup> 

<sup>a</sup>Department of Biosciences, College of Life and Environmental Sciences, University of Exeter, Exeter, UK; <sup>b</sup>Pollution Science Area, Centre for Ecology and Hydrology, Wallingford, Oxfordshire, UK

### ABSTRACT

The relative importance of ingestion and transdermal uptake of nanomaterials is poorly understood, particularly in sediment dwelling organisms, where diet has the potential to contribute significantly to particle accumulation. In aquatic sediments, nanoparticles may partition to bind with the solid fraction of sediment, be freely mobile in the pore water or, for certain metal/metal oxides, undergo dissolution, each of which could influence the route of nanoparticle uptake. Here, we used the freshwater worm *Lumbriculus variegatus* as a model species. We took advantage of its unique feeding and non-feeding life-stages to assess the contribution of dietary and transdermal uptake in the bioaccumulation of cerium oxide nanoparticles (CeO<sub>2</sub> NP) and soluble Ce(III)NO<sub>3</sub>. Distribution of cerium between the solid, colloidal and soluble fractions in the sediments was determined through sediment separations using micro and ultrafiltration techniques. We assessed particles of differing sizes (10, 28 and 615 nm CeO<sub>2</sub>) and stabilizing surfactants (10 nm electrostatic Citrate-CeO<sub>2</sub> and steric stabilized PEG-CeO<sub>2</sub>). Soluble Ce(III)NO<sub>3</sub> was found to accumulate readily across the skin of the worms whilst nanoparticles were not. Sediments reduced the uptake of Ce<sup>III</sup> by limiting the presence of dissolved species of cerium in the pore waters. Neither particle size nor the coatings studied altered the distribution of nanoparticles between solid and colloidal fractions of the sediment, with ~99% associated to the solid phase. Any uptake of CeO<sub>2</sub> nanoparticles into worms was only through ingestion. Stabilized 10 nm particles were retained even after gut clearance, indicating that these particles may translocate across the gut wall.

### ARTICLE HISTORY

Received 7 June 2018  
Revised 6 February 2019  
Accepted 5 March 2019

### KEYWORDS



Nanomaterial; bioaccumulation; ecotoxicology; *Lumbriculus variegatus*; dietary uptake

## Introduction

The versatility of engineered nanomaterials, where particle behavior may be tailored through alterations at the nanoscale, has led to an expansion of the technology into commercial applications including manufacturing, cosmetics, medicine and the textiles industry. The global nanomaterial industry is expected to reach US\$3 trillion by 2020 (Roco, Mirkin, and Hersam 2011), with the potential for 20 000 different NMs to be under development globally, based upon the sum of possible configurations of commonly used core elements, potential size and shape parameters and known surface coatings or other modifications, (Lynch 2016). An emerging body of scientific literature published over the last decade has found the potential for

engineered nanomaterials to exert toxicity upon a wide range of terrestrial (Tourinho et al. 2012; Simonin and Richaume 2015), marine (Baker, Tyler, and Galloway 2014), and freshwater aquatic species, (Vale et al. 2016) the underlying mechanisms of which are not yet fully understood.

Understanding biologically relevant fate processes of nanoparticles and the factors which determine bioaccumulation in different environmental compartments is essential for determining the risk that nanoparticles pose to the environment (Nam et al. 2014). Benthic species integral for ecosystem functioning (Lohrer, Thrush, and Gibbs 2004) are potentially, especially, vulnerable to exposure from engineered nanoparticles, as sediments are predicted to be a major sink of nanomaterials released

**CONTACT** Richard K. Cross  [R.Cross@exeter.ac.uk](mailto:R.Cross@exeter.ac.uk)  Pollution Science Area, Centre for Ecology and Hydrology, Wallingford, Oxfordshire OX10 8BB, UK  
Supplemental data for this article can be accessed [here](#).

© 2019 The Author(s). Published by Informa UK Limited, trading as Taylor & Francis Group

This is an Open Access article distributed under the terms of the Creative Commons Attribution License (<http://creativecommons.org/licenses/by/4.0/>), which permits unrestricted use, distribution, and reproduction in any medium, provided the original work is properly cited.

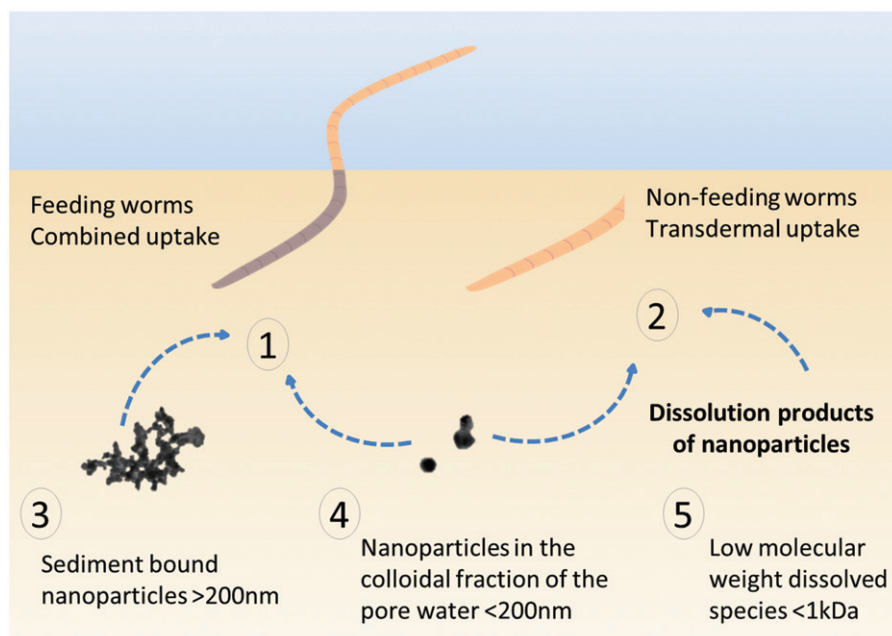


**Figure 1.** Schematic demonstrating different routes to uptake of nanoparticles in regrown worms (*Lumbriculus variegatus*) feeding upon sediment (1) exposed to a combination of dietary and transdermal uptake or non-feeding posteriors (2) exposed to transdermal uptake only. According to the method used to separate particles from sediment, those passing through a 1 kDa ultrafiltration process are defined as dissolved species (5), the colloidal pore water fraction <200 nm (4) and the remainder bound to the solid fraction of the sediment (3). Hypothesized routes to uptake of these three  $\text{CeO}_2$  fractions are proposed through dotted arrows.

into aquatic ecosystems. Heteroaggregation is a major driver of nanomaterial fate in aquatic environments under quiescent conditions leading to sedimentation and entry of engineered nanomaterials into sediment environments (Quik et al. 2012). Sediments may also then act as a source of nanomaterial release back into surface waters, for example through bioturbation or through scouring of the sediment bed in freshwater systems of high flow velocities (Dale, Lowry, and Casman 2015). This 'benthic-pelagic coupling' means sediment ecosystems are of concern both as a potential sink of engineered nanomaterials for future release, but also as an environment at risk of high exposure to these contaminants in their own right.

*Lumbriculus variegatus* is a freshwater sediment dwelling worm used in regulatory toxicity testing (OECD 2012) and in its natural environment may be exposed to contaminants both across the skin and through ingestion. Its wide distribution across North America and Europe means this species forms a major prey item in the aquatic food chain, with the potential for trophic transfer or biomagnification of contaminants. Mass balance studies in an estuarine mesocosm demonstrate that other low trophic level organisms such as clams and snails accumulate

engineered nanomaterials and act as an entry point into the wider food web (Ferry et al. 2009). The worm's unusual method of reproduction through architomy (Martinez, Reddy, and Zoran 2006), where fragmentation followed by segmental reorganization leads to the generation of feeding and non-feeding individuals, making it an ideal model to investigate the extent and route of uptake of nanoparticles from contaminated sediments. The posterior ends re-grow their anterior segments over a period of 7 to 10 days, during which ingestion of sediment material ceases (Leppänen and Kukkonen 1998). Generating these two phenotypes enables measurement of nanoparticle accumulation attributable to transdermal uptake in non-feeding worms (Figure 1.2) and combined transdermal and dietary uptake in feeding worms (Figure 1.1). This method has been used successfully to investigate the relative contribution of ingestion and transdermal uptake of pyrene (Leppänen and Kukkonen 1998) and ionizable pharmaceuticals including diclofenac and fluoxetine (Karlsson et al. 2016), but to our knowledge has never been used to examine the route to uptake of engineered nanoparticles.

Cerium oxide nanoparticles ( $\text{CeO}_2$  NPs) have been widely used in ceramics and glass polishing.

*In vitro*, cerium is able to generate radical oxygen species through a Fenton like reaction, redox cycling between the 3+ and 4+ states (Heckert, Seal, and Self 2008). Sublethal oxidative damage in the tissues of the marine sediment dwelling amphipod *Corophium volutator* exposed to CeO<sub>2</sub> NPs has been attributed to this redox cycling between Ce<sup>III</sup> and Ce<sup>IV</sup> at the nanoparticles surface *in vivo* (Dogra et al. 2016). Predicted environmental concentrations of these particles in surface waters are in the low µgL<sup>-1</sup> range (O'Brien and Cummins 2011), but CeO<sub>2</sub> has been demonstrated through both empirical and modeling studies to undergo rapid sedimentation in natural river waters (Quik, van De Meent, and Koelmans 2014). This has been ascribed to hetero-aggregation with natural colloids (Quik et al. 2012), and makes them a nanomaterial of potential concern in freshwater sediment systems. Being largely insoluble under most environmental conditions (Dahle, Livi, and Arai 2015) we utilized CeO<sub>2</sub> as a model nanomaterial for understanding nanoparticle fate and behavior in the absence of dissolution products during exposures.

Sediments present two potential routes to nanoparticle uptake in benthic species such as *L. variegatus*: (1) through ingestion of sediment bound nanoparticles and (2) via transdermal uptake from sediment pore waters and the overlying water (Cross, Tyler, and Galloway 2015). The contributions of these two routes for nanoparticle uptake may vary both with the physicochemical characteristics of the nanoparticles and the method of stabilization. Citric acid is a tricarboxylic acid, which behaves as a chelating ligand, adsorbing to Ce<sup>IV</sup> at the particle surface through bridging of the carboxylate group (Auffan et al. 2014), providing electrostatic stabilization to the particle. Polyethylene glycol (PEG) on the other hand forms a random hydrated hydrophilic coil at the particle surface, providing steric stabilization. Electrostatic and steric stabilization mechanisms have been demonstrated to result in different retentions in soils for silver nanoparticles (Hoppe et al. 2016) and to increase the persistence of nanoparticles in soil pore waters compared to their soluble counterparts (Whitley et al. 2013). Therefore, it was hypothesized that these different stabilization mechanisms would alter the partitioning of CeO<sub>2</sub> NPs between the solid (Figure 1.3), colloidal (Figure 1.4), and dissolved

phases of the sediment (Figure 1.5) and as such, influence the route to uptake and extent of their bioaccumulation.

Changing particle size may also alter how they interact at the nano-bio interface, with uptake through clathrin mediated endocytosis, a major mechanism for nanoparticle transport across cell membranes, reported to be optimal for the uptake of 50 nm nanoparticles (Kettler et al. 2014). As particle size increases between 200 and 500 nm, uptake into non-phagocytic cells may shift to caveolae-mediated endocytosis and this, in turn, can alter the cellular fate of the particles. Studies on non-phagocytic B16 cells have shown latex beads (500 nm) entering cells through caveolae-mediated endocytosis were not delivered to lysosomes, whereas they were for particles <200 nm entering cells through clathrin-mediated endocytosis (Rejman et al. 2004). As such, nanoparticle size may alter not only the route to cellular uptake at the nano-bio interface, but also how these particles are processed within the cells.

This study investigated the influence of particle coating and size on bioaccumulation using CeO<sub>2</sub> nanoparticles with a range of diameters between 4 and 615 nm and various stabilization mechanisms including uncoated, electrostatic and steric stabilization. Ce<sup>III</sup> was used to compare the route of uptake of soluble cerium with that of insoluble nanoparticles. The experimental design allows nanoparticle uptake to be discussed in the context of biologically relevant fate parameters, including persistence of nanoparticles as colloidal (Figure 1.4) or dissolved species in the pore waters (Figure 1.5). From a whole organism perspective, the route of nanoparticle uptake could alter their systemic fate within an organism, with implications for the nanomaterial's toxicity or site of action. For example, nanomaterials internalized through dietary uptake will come into contact with different organs and structures within the organism than those in contact with the skin. Whilst the potential implications of different routes of nanomaterial uptake are great for both bioaccumulation and toxicity of these materials, it presents a significant gap in our knowledge. This study aims to address this gap in our understanding, focussing on the fate of nanoparticles in sediments and the role this has on nanoparticle route of uptake.

## Methods

Batch sediment experiments were conducted to assess partitioning of cerium between the solid, colloidal, and dissolved low molecular weight fraction (LMW) of the sediment to provide context on the fate and behavior of nanomaterials during biological exposures. The biological exposures assessed differences in uptake of dissolved  $\text{Ce}^{\text{III}}$  compared to  $\text{CeO}_2$  NPs and assessed the role of nanoparticle size and stabilizing coatings on the route and extent of uptake of  $\text{CeO}_2$ -NPs from sediments.

### Materials and characterization of pristine particles

$\text{CeO}_2$  reference materials NM211, NM212 and NM213 (JRC, Italy) (Singh et al. 2014) are reported here with reference to their primary particle size as  $\text{CeO}_2$ -10,  $\text{CeO}_2$ -28 and  $\text{CeO}_2$ -615. Two commercial 4–8 nm  $\text{CeO}_2$  nanoparticles (PlasmaChem, Germany) were provided as part of the GUIDEnano project (<http://www.guidenano.eu/>): electrostatically stabilized Citrate- $\text{CeO}_2$  and sterically stabilized mono polyethylene glycol phosphonic acid ester  $\text{CeO}_2$  (PEG- $\text{CeO}_2$ ).  $\text{Ce}(\text{III})\text{NO}_3$  salt, 99.999% purity (Sigma Aldrich, UK) was used as a soluble source of  $\text{Ce}^{\text{III}}$ .

Characterization of particle size and stability (Supporting Information SI 2) used Transmission Electron Microscopy (TEM), Scanning Electron Microscopy (SEM), and Dynamic Light Scattering (DLS). Characterization and exposures occurred in 'ultrapure' water ( $18 \Omega \text{ cm}^{-1}$ , Millipore) or 'freshwater' (pH  $7.75 \pm 0.03$ , conductivity  $715 \mu\text{Scm}^{-1} \pm 11.1 \mu\text{Scm}^{-1}$ , calculated ionic strength  $13.4 \text{ mmolL}^{-1}$ ), a reconstituted hard water described in OECD TG315 (OECD 2008). Visual MINTEQ modeling the speciation of  $\text{Ce}(\text{III})\text{NO}_3$  in freshwater is presented in Supporting Information SI 3.

The standard soil LUFA Speyer 2.4 (LUFA Speyer, Germany; organic carbon, 2.03%; particle size distribution  $<0.002 \text{ mm}$ , 25.8%) was used as a model sediment for consistency between exposures. Additional properties of LUFA Speyer 2.4 provided by the supplier are detailed in Supporting Information SI 7. Water, tissue and sediment samples were microwave digested before analysis with *aqua regia*, a 1:4 mix of TraceSELECT® grade nitric acid and hydrochloric acid (Sigma-Aldrich, UK).

Elemental cerium was measured using Inductively Coupled Plasma Mass Spectrometry (Thermo Scientific X Series 2 ICP-MS, Hemel Hempstead, UK).

### Preparation of nanoparticle stocks and dispersions

$\text{CeO}_2$ -10,  $\text{CeO}_2$ -28 and  $\text{CeO}_2$ -615 particles are dry powders so were dispersed following the PROSPECT protocol (Prospect 2010). Weighed powders were wetted drop wise to a paste, diluted to concentration then sonicated on ice for 2 min at 80% intensity to de-agglomerate the dispersion using a High Intensity Ultrasonic Processor (Sonics, USA).

PlasmaChem particles provided in dispersion were homogenized through gentle overhead mixing to avoid damage and destabilization of the nanoparticle coatings. Stocks and working solutions for these nanoparticles were prepared by dilution in the relevant media.

### Fate of $\text{CeO}_2$ NPs in freshwater

DLS (Malvern Instruments, Zetasizer nano Z-S) with a wavelength of 663 nm using Noninvasive Backscatter optics and a scattering angle of  $173^\circ$  measured particle size and zeta-potential to semi-quantitatively examine stability and agglomeration in ultrapure and freshwater over the biological exposure period. Details of how stability and agglomeration state were measured are presented in Supporting Information SI 4, with results presented in Supporting Information SI 5.

### Fate of $\text{CeO}_2$ NPs in the solid bound, colloidal and dissolved low molecular weight fractions of the sediment

The colloidal and dissolved low molecular weight fraction (LMW-Ce) of the sediment pore waters were separated through a combination of centrifugation and micro/ultra-filtration techniques (Cornelis et al. 2010). A 1:10 dilution of 6 day aged contaminated sediment in freshwater was mixed for 6 h at  $20^\circ \text{C}$  in the dark, before centrifugation at  $2300 g$  for 15 min. The supernatant was micro-filtered to  $<200 \text{ nm}$  (GE Whatman, USA) defining the colloidal Ce in the pore waters, whilst dissolved LMW-Ce  $<1 \text{ kDa}$  was separated using ultrafiltration

centrifugation (Microcep™, Pall, USA) at 4000 *g* for 15 min. Filters were preconditioned to limit losses of nanoparticles to the filtration membranes using 0.1 M copper nitrate (Cu(NO<sub>3</sub>)<sub>2</sub>·3H<sub>2</sub>O, Sigma Aldrich, UK).

### **Generating feeding and non-feeding worm phenotypes**

*Lumbriculus variegatus* (Blades Biological UK Ltd., UK) were housed on clean silica sand under an aerated artificial freshwater flow through system (pH 7.6, conductivity 360 µS cm<sup>-1</sup>). Organisms were fed twice weekly with 0.5 g ground fish food (TetraMin, Blacksburg, USA).

All worms were acclimated for 10 days on clean sediment prior to exposure. Feeding organisms were split by scalpel at the midpoint at the start of the acclimation phase (Supporting Information SI 1. a) to synchronize the worms and ensure no natural splitting and cessation of feeding would occur during the exposures (Leppänen and Kukkonen, 1998). Non-feeding groups were also acclimated, feeding on clean sediments for 10 days (Supporting Information SI 1.b) before synchronization immediately prior to their addition to the exposure units (Supporting Information SI 1.c). Examples of organisms at each life stage (Supporting Information SI 6) were imaged using a QIClick™ CCD Camera (QImaging, Canada) mounted to an LTSu-1000 light microscope (Labtech International Ltd, UK).

### **Waterborne exposures to soluble Ce<sup>III</sup>**

Waterborne exposure to Ce(III)NO<sub>3</sub> examined the potential for transdermal uptake of dissolved forms of Ce<sup>III</sup> in model sediment pore waters, in the absence of solid constituents of the sediment. Each static, 24 h freshwater exposure was conducted in multiwall polystyrene culture plates (Grenier, Austria), in the artificial freshwater.

Cerium exposures were randomized in 10 ml wells with *n* = 3 per treatment, each comprising of 3 randomly assigned individuals pooled per test unit. Ce<sup>III</sup> was spiked as cerium nitrate at two concentrations calculated as 11.3 mgL<sup>-1</sup> and 11.3 µgL<sup>-1</sup>. The high concentration was selected to represent similar orders of magnitude exposures to the total Ce spiked to sediments. The water holding capacity of the soil

substrate was 0.441 mg g<sup>-1</sup> meaning 11.3 mgL<sup>-1</sup> would be equivalent to 5 mgkg<sup>-1</sup> spiked to sediment. The lower concentration was representative of the low µgL<sup>-1</sup> dissolved Ce concentration detected in the pore waters in Ce<sup>III</sup> sediment exposures, whilst still being sufficient to result in appreciable uptake of Ce during the acute exposures. These are not representative of environmental concentrations of soluble cerium, but rather act as upper and lower bounds for comparison of the route of uptake of soluble forms of cerium as opposed to nanoparticulate CeO<sub>2</sub>. No mortality occurred in any treatment.

### **The role of particle size, solubility and surface coating on the route and extent of uptake of cerium from sediments**

Static sediment exposures were performed in acid washed 50 ml polypropylene CELLSTAR tubes (Greiner Bio-One, UK) to limit adsorption of nanoparticles to surfaces (Hammes, 2012). Each unit comprised of 5 pooled individuals within 10 g of sediment, with 40 ml aerated overlying freshwater (*n* = 5 per treatment). Nanoparticles (CeO<sub>2</sub>-10, CeO<sub>2</sub>-28, CeO<sub>2</sub>-615, Citrate- and PEG coated CeO<sub>2</sub>) dispersed in freshwater were wet-spiked and mixed into the sediment to saturation, at a calculated loading of 50 mgkg<sup>-1</sup> elemental Ce. Ce(III)NO<sub>3</sub> was spiked to the sediment in ultrapure water to ensure Ce was initially in the dissolved Ce<sup>III</sup> form upon introduction to the sediments. Exposure conditions and validity of the test was in accordance with OECD TG315 (OECD 2008). Sediments settled for 24 h before worms were randomly allocated to exposure units. Negligible cerium partitioned to the overlying water after settling (between 0.001–0.03%). Temperature was controlled throughout the experiment at 20 °C ± 2 °C under a light-dark rotation of 16:8 h.

After 5 days, all organisms were removed from the test units through gentle resuspension of the sediments with freshwater. Organisms without a clearance phase were rinsed in freshwater (Supporting Information SI 1.d), snap frozen in liquid nitrogen and stored at -80 °C. Remaining worms were allowed to evacuate their gut contents over a period of 6 h in freshwater (Supporting Information SI 1.e), sufficient to remove >98% of the gut contents (Mount, Dawson and Burkhard, 1999), with three water changes to avoid re-

ingestion of eliminated particles and were then snap freezing and stored at  $-80^{\circ}\text{C}$ . All tissues and sediment samples were freeze dried and weighed (Christ Freeze Dryer, Beta LD plus 2-8).

Freeze-dried tissues and sediments were microwave digested in *aqua regia* (Ethos EZ, Milestone, USA) following the Ethos EZ recommended procedures. Total Ce concentration was measured using ICP-MS. Procedural blanks were analyzed during each digestion run and spike recoveries performed in sediments. Recoveries for  $\text{CeO}_2$  from sediments ranged from 87.6% to  $\sim 100\%$  after microwave digestion in *aqua regia*.

### Data handling and statistical analysis

All statistical analysis was performed in R (RStudio Team, 2015). A minimum adequate model approach was taken and appropriate *post hoc* tests based upon results from factorial design two-way analysis of variance (ANOVA). Where assumptions of normality or homoscedasticity were not met, relevant transformations to the data were performed. Tukey's HSD *post hoc* was used where body burdens differed significantly either between cerium treatments (treatment effect) or where cerium was accumulated through different routes to uptake, for example if uptake was greater in feeding organisms than non-feeding organisms (organism group effect). In some cases the route to uptake differed significantly between cerium treatments (interaction effect). Where this interaction effect between nanoparticle treatment and route to uptake was significant, pairwise contrasts were performed using the least-squares means approach with Tukey's method for *p*-value adjustment (LSM Tukey's method). Graphs present means, standard errors and statistically significant differences, with significance taken as  $p < 0.05$ .

## Results

### Fate and characterization of $\text{CeO}_2$ in sediments

For all  $\text{CeO}_2$  exposures, LMW-Ce was below the limit of detection (LOD) of ICP-MS (Table 1). LMW-Ce was only detected in  $\text{Ce}^{\text{III}}$  treatments at a very low concentration of  $0.87 \mu\text{gkg}^{-1}$  ( $\sim 0.002\%$  of total Ce). The majority of Ce in all treatments was bound to the solid fraction of the sediment ( $\sim 99\%$ ), but for all treatments a fraction of colloidal

nanoparticles persisted in the pore waters above that found in the controls ( $p < 0.05$ , Dunnett's test). Citrate- $\text{CeO}_2$  had significantly higher colloidal concentrations than all other treatments ( $p < 0.05$ , Tukey's HSD) but was still low compared with that associated with the sediment (98.8%).

### Stability and agglomeration of $\text{CeO}_2$ nanoparticles over time

Detailed characterizations of the NPs in ultrapure and freshwater across the exposure period are presented in Supporting Information SI 5. In freshwater both particles agglomerated. PEG- $\text{CeO}_2$  was less stable than Citrate- $\text{CeO}_2$ , with rapid agglomeration to sizes  $>1000$  nm and sedimentation within 24 h. In ultrapure water, 10.5 nm (Citrate- $\text{CeO}_2$ ) and 14.8 nm (PEG- $\text{CeO}_2$ ) particles remained in dispersion, indicating these materials can persist as individual, stabilized nanoparticles. In freshwater, these small particles were no longer detectable, an artifact possibly due to the exponential relationship between particle size and DLS signal intensity which could mean the presence of larger aggregates formed in freshwater masked the lower signal from individual particles persisting in dispersion (Supporting Information SI 5 B and D).

### Route of uptake of dissolved cerium from waterborne exposures

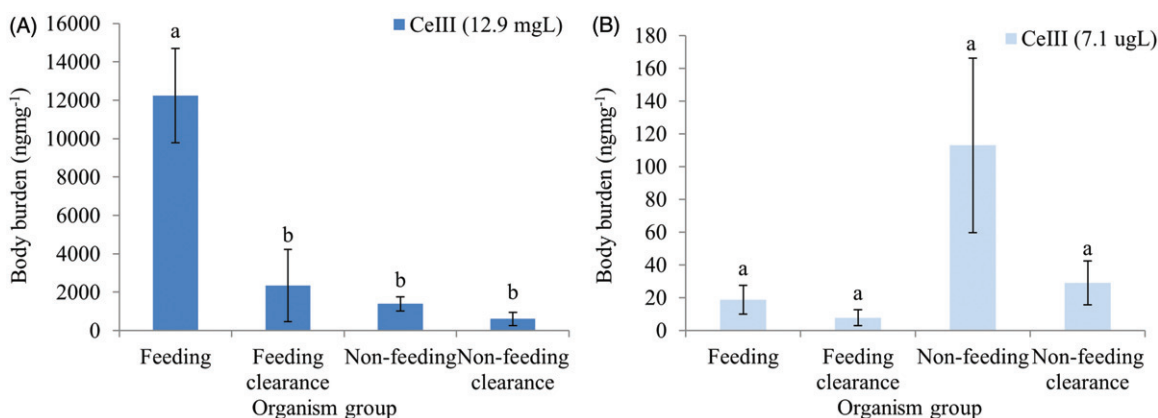
Modeling speciation of  $\text{Ce}(\text{III})\text{NO}_3$  in freshwater found all species to be below saturation (Supporting Information SI 3).  $\text{CeCO}_3^+$  was most abundant in freshwater, ranging between 58.55 and 77.164% of the total Ce whilst dissolved  $\text{Ce}^{\text{III}}$  made up 22.13% of the high concentration exposure and 6.45% in low exposure.

Measured exposure concentrations were  $12.9 \pm 0.09 \text{ mgL}^{-1}$  and  $7.1 \pm 0.007 \mu\text{gL}^{-1}$ , in reasonable agreement with the expected doses. Body burdens of Ce were  $< \text{LOQ}$  (limit of quantification) in controls therefore all uptake of Ce during exposure to  $\text{Ce}(\text{III})\text{NO}_3$  was significant in exposed worms. Data for exposed worms was non-normal for both experiments, so body burdens were log-transformed.

Under the high level exposure regime (Figure 2(A)), transdermal uptake accounted for Ce body burdens between  $0.6$  and  $2.3 \mu\text{gmg}^{-1}$  in non-

**Table 1.** Partitioning of cerium between the solid, colloidal and low molecular weight fraction of the sediment at the end of the 5 day biological exposure.

Treatment	Sediment Ce mgkg <sup>-1</sup>	Colloidal fraction <200 nm mgkg <sup>-1</sup> (s.e.)	Dissolved species of Ce
			LMW-Ce <1 kDa mgkg <sup>-1</sup>
CeO <sub>2</sub> -10 (10-20 nm)	34.86	0.0255 (0.013)	<LOD
CeO <sub>2</sub> -28 (28.4 nm)	31.66	0.0851 (0.035)	<LOD
CeO <sub>2</sub> -615 (615.3 nm)	19.33	0.2178 (0.138)	<LOD
Citrate-CeO <sub>2</sub> (4-8 nm)	56.57	0.674 (0.058)	<LOD
PEG-CeO <sub>2</sub> (4-8 nm)	59.03	0.075 (0.005)	<LOD
Ce(NO <sub>3</sub> ) <sub>3</sub>	43.62	0.0106 (0.0001)	0.00087
Control	43.59	0.0051 (0.003)	<LOD

**Figure 2.** Body burdens (ngmg<sup>-1</sup> Ce) in worms exposed for 24 hours to 12.9 mgL<sup>-1</sup> (A) or 7.1 µg L<sup>-1</sup> Ce<sup>III</sup> (B) dosed as cerium nitrate (Ce<sup>III</sup>NO<sub>3</sub>) in freshwater ( $n = 3$ ). Different letters within each frame denote a significant difference between levels of organism group (Tukey's HSD,  $p < 0.05$ ).

feeding worms and feeding worms that had undergone gut clearance ( $p = 0.277$ , Tukey's HSD). Elevated Ce in feeding organisms that occurred via imbibed fluid ( $p = 0.022$ , Tukey's HSD) was lost after clearance.

In the low exposure (Figure 2(B)), there was no statistically significant difference between organisms in the different treatment groups ( $p = 0.667$ , ANOVA) indicating transdermal accumulation accounted for all uptake of Ce. Non-feeding worms without a clearance phase had high but variable body burdens, at  $112.95 \pm 53.3$  ngmg<sup>-1</sup>. All other groups had body burdens ranging between 7.7 and 28.9 ngmg<sup>-1</sup>.

#### Effects of size and solubility on bioaccumulation of cerium from sediments

No uptake of Ce was quantifiable in tissues of non-feeding worms exposed to CeO<sub>2</sub>-10, CeO<sub>2</sub>-28, nor

non-exposed control worms (Figure 3). This indicates transdermal uptake did not occur for these nanoparticles. Of the non-feeding worms, only those exposed to Ce<sup>III</sup> had body burdens of Ce above the LOQ, indicating some transdermal uptake of Ce during exposure to soluble Ce<sup>III</sup>. The Ce taken up across the skin during Ce<sup>III</sup> exposure was lost during the clearance phase, reducing body burdens to < LOQ. Body burdens of Ce in feeding worms during exposure to CeO<sub>2</sub>-10, CeO<sub>2</sub>-28 and Ce<sup>III</sup> in sediments did not conform to assumptions of normality, so data was log-transformed.

Significant uptake was measured for feeding worms exposed to all forms of engineered Ce compared with non-exposed controls before gut clearance ( $p < 0.001$ , LSM Tukey's method). After 6 h gut clearance body burdens were significantly reduced for all three cerium exposures ( $p < 0.001$ , LSM Tukey's method). Body burdens remained significantly higher in Ce<sup>III</sup> exposed worms after clearance ( $p = 0.0007$ , LSM Tukey's method), indicating significant accumulation. CeO<sub>2</sub>-28

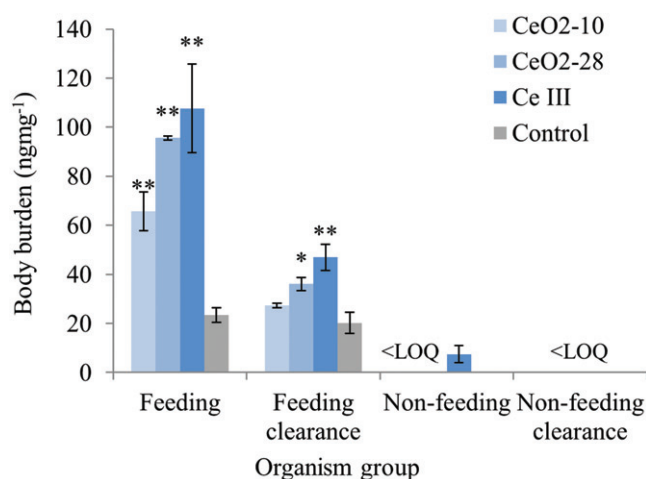


**Figure 3.** Body burdens ( $\text{ngmg}^{-1}$  Ce) in organisms exposed to sediments contaminated with  $\text{CeO}_2$  NPs of varying size, and to dissolved  $\text{Ce}^{\text{III}}$  ( $n = 3$ ). Body burdens of Ce greater than in control organisms is denoted by an asterisk (\*  $p < 0.05$ , \*\*  $p < 0.001$ ).

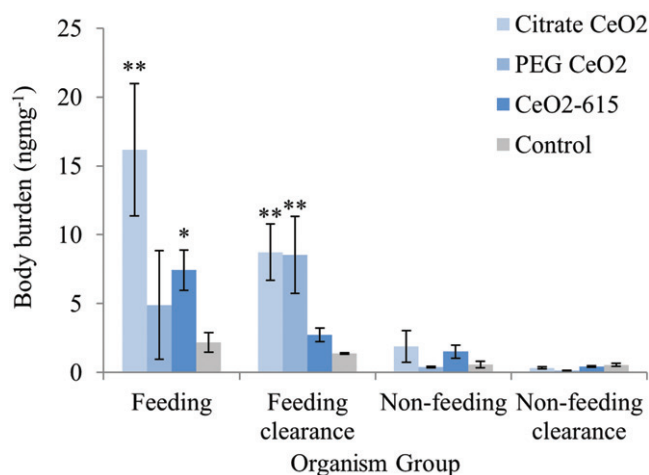


**Figure 4.** Body burdens ( $\text{ngmg}^{-1}$ ) for organisms exposed to Citrate- $\text{CeO}_2$ , PEG- $\text{CeO}_2$  or  $\text{CeO}_2$ -615. Body burdens significantly higher than in non-exposed control organisms are denoted by an asterisk (\*  $p < 0.05$ , \*\*  $p < 0.001$ ).

was also retained after gut clearance but the accumulation above background levels was less pronounced ( $p = 0.0311$ , LSM Tukey's method).  $\text{CeO}_2$ -10 was lost to the extent body burdens were no longer significantly higher than controls after evacuation of the gut contents ( $p = 0.346$ , LSM Tukey's method) and so were not considered accumulated.

#### **The effect of surface coatings on accumulation of $\text{CeO}_2$ dosed in sediments**

Data for body burdens were non-normally distributed so were log transformed. ANOVA found a significant interaction effect between the nanoparticle

exposure and the organism group ( $p < 0.05$ ). This indicates that body burdens differed significantly between organism groups and that these differences were not the same for each cerium exposure. Calculated body burdens were generally lower in this experiment than those found in Figure 3, due to inter-experimental variation in tissue mass. Tissue mass of pooled individuals were greater during the experiment presented in Figure 4.

Feeding organisms had greater body burdens of cerium when exposed to Citrate- $\text{CeO}_2$  and  $\text{CeO}_2$ -615 before the gut clearance phase ( $p < 0.05$ , LSM Tukey's method). This represents cerium associated with material within the guts or loosely



adsorbed to external membranes. Upon removal of this material during the clearance phase, Ce body burdens in each nanoparticle treatment remained significantly greater than in non-exposed controls ( $p < 0.001$ , LSM Tukey's method). However, body burdens of CeO<sub>2</sub>-615 fell during this clearance phase and were no longer significantly different from the body burden of Ce in non-exposed control organisms ( $p = 0.288$ , LSM Tukey's method). Body burdens for all non-feeding organisms exposed to cerium were no different from those of non-exposed controls, indicating that transdermal uptake was not possible for these particles ( $p > 0.05$ , LSM Tukey's method).

## Discussion

### *Coated nanoparticles were destabilized over time in freshwater representing sediment pore waters*

Measuring stability and agglomeration of Citrate- and PEG-CeO<sub>2</sub> in water dispersions demonstrated that some stabilized primary sized CeO<sub>2</sub> particles (10–15 nm) can remain in dispersion in water for periods up to 6 days (Supporting Information SI 5). However, the majority of particles agglomerated in freshwater, which is likely to reduce their mobility in sediments through physical straining of larger agglomerates. The positive or neutral Zeta potential of CeO<sub>2</sub>-10, CeO<sub>2</sub>-28 and CeO<sub>2</sub>-615 explains the strong associations of these particles to the predominantly negative charged solid fraction of the sediment (>99% sediment bound) and their instability in freshwater.

Coated particles were also destabilized in freshwater. Zeta potential of Citrate-CeO<sub>2</sub> was  $-15.7$  mV in freshwater compared to  $-37.9$  mV in ultrapure water. Likewise, PEG-CeO<sub>2</sub> had a zeta potential of  $-48.9$  mV in ultrapure water, but only  $-16.5$  mV in freshwater. This resulted in aggregation/agglomeration and subsequent sedimentation of particles (Supporting Information SI 5 B and D). Whilst such data must be treated with caution as to the absolute values calculated, qualitatively this demonstrates the instability of CeO<sub>2</sub> in freshwater. This has implications for their mobility in sediment pore waters, as aggregation would lead to straining as these aggregates reach sizes in the micrometre range (Sang et al. 2013).

### *Size and surface functionalization did not appreciably alter distribution of CeO<sub>2</sub> nanoparticles between the solid bound, colloidal and LMW fractions of the sediment*

Direct measurement of the size distributions of the nanomaterials could not be performed in the isolated pore waters due to the inability of DLS to distinguish between material types. Therefore, the concentration of cerium detected in the colloidal and LMW fractions of the sediment pore waters was measured as an indicator of the fate of these materials during the biological exposures. All forms of CeO<sub>2</sub> were predominantly immobile ( $\sim 99\%$  associated with the solid fraction of the sediment) and did not dissolve irrespective of their size or surface coating (Table 1), in agreement with previous studies (Cornelis et al. 2011; Liu, Chen, and Su 2012). A small concentration of dissolved Ce was detectable in the pore waters of sediments spiked with soluble Ce(III)NO<sub>3</sub>,  $<0.01\%$  of the initial dose at  $\sim 0.867 \mu\text{gkg}^{-1}$  and a colloidal concentration of  $10.6 \mu\text{gkg}^{-1}$ , similar to that of nanoparticulate CeO<sub>2</sub>. The positive Zeta potential (Supporting Information SI 2) for CeO<sub>2</sub>-10, CeO<sub>2</sub>-28 and CeO<sub>2</sub>-615 is likely to lead to rapid association with the predominantly negatively charged components of the sediment. In freshwater, coated CeO<sub>2</sub> nanoparticles also underwent aggregation, reaching sizes of  $>200$  nm (Supporting Information SI 5.B and D), which would exclude the majority from the colloidal fraction of the sediments we examined ( $<200$  nm).

Negatively charged stabilized CeO<sub>2</sub> could also undergo heteroaggregation with organic matter or to positively charged edges in lattice layer clays (Cornelis et al. 2011). During sediment exposures, pH of the overlying water was  $7.75 \pm 0.03$  whilst pore water pH was  $7.45 \pm 0.01$ . Under these conditions clays would likely retain their overall negative charge (Tombácz and Szekeres 2004). However, the relatively high ionic strength of the pore water of  $\sim 0.01$  M during these exposures would lead to a compression of the electric double layer extending from negatively charged surfaces, lowering the interaction energy barrier which attractive van der Waals forces must overcome for aggregation. This would allow deposition of nanoparticles onto sediment colloids (Sang et al. 2013) similar to the

behavior observed for 30 nm TiO<sub>2</sub> and its heteroaggregation with clay (Labille et al. 2015). Indeed, the capacity for higher ionic strength water to increase heteroaggregation of CeO<sub>2</sub> with natural colloids has been demonstrated in estuarine water (Quik, van De Meent, and Koelmans 2014). Such processes meant nanoparticle size or form of surfactant had little influence over the total distribution of CeO<sub>2</sub> NPs between the solid and colloidal phase of the sediments during our study. Instead, conditions within the sediment appeared to negate any differences in overall partitioning that could arise from differences in size or surface coatings of the nanoparticles.

This has wider implications for our approach to assessing the bioavailability and bioaccumulation of engineered nanomaterials from sediment environments. It is widely acknowledged that the fate of nanomaterials is dependent on the conditions of the surrounding environmental matrix. Efforts have been made to establish a suite of representative artificial freshwaters which cover the range of conditions present across European surface waters (Hammes, Gallego-Urrea, and Hassellöv 2013). Whilst such information is not yet available for sediment systems, evidence from fate studies in saturated terrestrial soils indicate that the mobility and dissolution of inorganic engineered nanomaterials such as silver is influenced by soil pH, ionic strength of the pore waters, the presence of organic matter and the clay content of natural soils (Cornelis et al. 2012). Presence of natural colloids was also highlighted as of importance in determining the retention of 20 nm CeO<sub>2</sub>-NPs in suspensions of natural soils (Cornelis et al. 2011). Bioavailability of nanomaterials can be related to their mobility and interactions with solid phases of sediments (Cornelis et al. 2014). The current study demonstrates that the distribution of CeO<sub>2</sub> between the colloidal and solid bound fractions of the sediment was not sufficiently altered by intrinsic properties of either primary particle size or surface coating to result in differences in the route to uptake of these nanoparticles. Future consideration must be made as to whether sediment chemistry may alter the fate of these nanomaterials sufficiently to result in increased bioaccumulation.

### ***Dissolved species of Ce<sup>III</sup> are accumulated through both ingestion and transdermal uptake from waterborne exposures***

Worms were exposed in freshwater for 24 h to two concentrations of Ce<sup>III</sup> spiked as Ce(III)NO<sub>3</sub> representing concentrations of similar magnitude to the total Ce concentration in the sediments and the dissolved Ce detected in the pore waters. Both exposures resulted in significant uptake of Ce compared to non-exposed freshwater controls (where body burdens were <LOQ), predominantly through transdermal uptake. At the higher exposure concentration, it should be noted that some worms produced a mucus layer in response to the cerium treatment. Under the high concentration exposure, imbibed fluid contributed towards body burdens in feeding worms with a functioning anterior, which was then lost through purging the gut. As there was no difference between feeding worms which have undergone a period of non-exposure (clearance) and non-feeding worms, we conclude that assimilation of Ce within the gut over this short exposure does not contribute significantly to body burdens. As such, body burdens between 0.6 and 2.3 µgmg<sup>-1</sup> Ce can be attributed to transdermal uptake or associations of Ce with external surfaces of the worms.

In the lower 7.1 µgL<sup>-1</sup> exposure differences between organisms in the different treatment groups were indistinguishable. Therefore, all Ce accumulation was considered attributable to transdermal uptake. MINTEQ modeling (Supporting Information SI 3) predicts a significant proportion of Ce in the Ce<sup>III</sup> form, 22.13% and 6.449% respectively for the high and low concentration exposures. Dissolved Ce<sup>III</sup> can act as a Lewis-acid, orientating towards Lewis-base OH<sup>-</sup> in cell plasma membrane proteins. This has been demonstrated by the targeting of Ce<sup>III</sup> to cell plasma membrane proteins in horseradish and uptake into cells exposed at high µM concentrations (Yang et al. 2012). The Ce<sup>III</sup> then forms a Lewis acid-base adduct, with the oxygen donating a lone electron pair to the Ce<sup>III</sup>, resulting in a single reaction product. The effect of this within biological systems is that dissolved Ce ions experience slower elimination from the blood and accumulation in the skeleton, liver, kidneys and gastrointestinal tract of rats intravenously injected with cerium chloride (Yokel et al. 2014). This Lewis

acid-base type reaction may be responsible for apparent transdermal accumulation of dissolved Ce in non-feeding worms alongside movement along diffusion gradients; however, future work would need to investigate the exact mechanism of uptake.

An important implication of this finding is that low molecular weight species resulting from dissolution of a nanomaterial may result in an additional route to uptake of the element form of the contaminant, compared with the nanoparticulate form of the material, through dermal uptake into sediment dwelling species. Consideration for the wider risk assessment of engineered nanomaterials in sediment systems should focus on the different hazardous effects that ingested nanomaterials may induce as compared to soluble counterparts accumulated through transdermal uptake. Developing our understanding in this area could lead to safer-by-design strategies for nanomaterials expected to enter sediment ecosystems, which could mitigate/prevent nanomaterial behaviors that lead to specific routes to uptake, so as to reduce their potential for internalization and toxicity.

### ***The role of size and dissolution on bioaccumulation of cerium from sediments***

Transdermal uptake of non-stabilized CeO<sub>2</sub>-10 and CeO<sub>2</sub>-28 did not occur, whereas ingestion of CeO<sub>2</sub> as part of a sediment diet was possible. There was no difference in the distribution of these different materials between colloidal and solid phases of sediments and no difference in the extent of their initial uptake (before gut clearance) between nanoparticle treatments. The high affinity of the CeO<sub>2</sub> NP to the solid fraction of the sediment means that the ingestion of these particles and their subsequent availability will be a function of this distribution between the solid and colloidal phases of the sediment, and the particle size of those NPs that exist in the colloidal fraction of the sediment pore waters. This indicates that sediment properties are primarily responsible for determining the total ingestion of the CeO<sub>2</sub>, not the properties of the particles themselves.

Feeding worms exposed to both nanoparticles exhibited body burdens greater than in controls before gut clearance; however, this was significantly reduced upon clearance (Figure 3). This indicates a

significant proportion of this body burden was attributable to CeO<sub>2</sub> associated with ingested sediment material. For organisms exposed to CeO<sub>2</sub>-10, body burdens were reduced to the level of that in non-exposed controls after gut clearance. Body burdens of CeO<sub>2</sub>-28 were significantly reduced but remained higher than in controls. This suggests that there could be some translocation of Ce within the guts upon exposure to CeO<sub>2</sub>-28. Future investigations could use a combination of imaging and spectrometry techniques to visualize this translocation across the gut. Transmission electron microscopy coupled to energy dispersive x-ray spectrometry (TEM-EDX) has successfully visualized AgNPs associated with the apical plasma membrane, in endocytotic pits and in endosomes in the gut of the estuarine polychaete *Nereis diversicolor* (García-Alonso et al. 2011). Coherent anti-stokes Raman scattering microscopy (CARS) has also been successfully employed to visualize localization of ingested TiO<sub>2</sub>-NP aggregates in the lumen of the gut of the estuarine worm *Arenicola marina* (Galloway et al. 2010).

CeO<sub>2</sub>-10 and CeO<sub>2</sub>-28 had a Zeta-potential in ultrapure water of +28 and +33 mV, respectively. Alumina clays are abundant in sediments and are largely negatively charged due to isomorphous substitution of a single Si<sup>4+</sup> with Al<sup>3+</sup> in the neutrally charged Si<sub>2</sub>O<sub>4</sub> quartz crystal to form the clay SiAlO<sub>4</sub><sup>-</sup>. Binding of positively charged uncoated CeO<sub>2</sub> nanoparticles to these negative charged sites, which will be abundant in the clayey loam LUFA Speyer 2.4 (Supporting Information SI 7), could prevent dissociation of CeO<sub>2</sub> within the worms upon ingestion. Indeed, investigation into the adsorption of CeO<sub>2</sub> nanoparticles of similar size to those studied in this article (<25 nm) in model saturated soils, demonstrated greater attachment of the nanomaterials to kaolin clay than sand particles in batch experiments (Zhang et al. 2018). Positively charged CeO<sub>2</sub> also had greater attachment to kaolin clays than negatively charged forms, attributed to physical adsorption processes through electrostatic interactions. This may have implications for bioavailability and may explain the lower bioavailability of the uncoated positively charged CeO<sub>2</sub> in this study, explaining the limited subsequent uptake of uncoated, positively charged CeO<sub>2</sub> across the gut epithelia. Size distribution measured by DLS

and centrifugal liquid sedimentation in various freshwater and marine media demonstrates that aggregates formed of CeO<sub>2</sub>-28 are consistently smaller than those formed from CeO<sub>2</sub>-10 (Singh et al. 2014). This could also play a role in the difference observed in uptake of CeO<sub>2</sub>-28 compared with CeO<sub>2</sub>-10.

Exposure to Ce<sup>III</sup> on the other hand did result in significant transdermal and dietary uptake of Ce, in agreement with the transdermal uptake observed in waterborne exposures (Figure 2). In sediments, transdermal uptake was only significant for non-feeding organisms before the clearance phase. Uptake was also lower from sediments (7.9 ngmg<sup>-1</sup>) compared to in freshwater (2.3 μgmg<sup>-1</sup>) when exposed to similar total concentrations of Ce(III)NO<sub>3</sub>. Sediments, therefore, reduced the availability of dissolved cerium to the organism, reducing the concentration of free dissolved species of cerium in the pore waters to <0.01% of the original concentration. However, an interesting observation of this study is that, whilst nanoparticulate forms of CeO<sub>2</sub> were only internalized through ingestion, the soluble counterpart (Ce(III)NO<sub>3</sub>) could experience combined accumulation of cerium through both ingestion and transdermal uptake.

***Stabilized nanoparticles were accumulated through diet from sediments, but surface functionalisation does not alter the extent of their uptake***

After a gut clearance phase, Citrate- and PEG-CeO<sub>2</sub> nanoparticles with a primary particle size between 4–8 nm were retained in feeding worms, but this was not the case for bulk-sized CeO<sub>2</sub>-615 (Figure 4). This suggests that translocation and accumulation of the small stabilized CeO<sub>2</sub> NPs was possible within the gut, but that such translocation did not occur for bulk CeO<sub>2</sub>-615. This may be due to physical constraints of the larger CeO<sub>2</sub>-615 meaning the lumen of the gut acted as an effective barrier to its uptake as passive mechanisms of nanomaterial transport such as diffusion and persorption occur more rapidly for smaller nanomaterials (Cornelis et al. 2014), whilst endocytosis appears to have an optimum efficiency for nanoparticles around 50 nm (Kettler et al. 2014). Stabilization of NPs allowed for potential translocation of CeO<sub>2</sub> across the gut, however,

the mechanism of stabilization did not appear to alter the overall uptake of Citrate- or PEG-CeO<sub>2</sub>, with similar body burdens accumulated of both nanoparticles after gut clearance. Whilst uptake of particles <10 nm in size is greater than that of its bulk CeO<sub>2</sub> counterpart, we have demonstrated that in sediment environments the potential for biomagnification of nanoparticulate cerium is low.

Interestingly, some of the increase in body burdens of Ce in feeding worms exposed to cerium compared to non-exposed control worms could be attributed to material in the guts, which was then lost during the 6 hour clearance phase. This was particularly true of Ce10 and bulk CeO<sub>2</sub>-615, where the loss of Ce during the clearance phase resulted in body burdens no different from non-exposed controls. In these treatments, CeO<sub>2</sub> could not be said to have accumulated through ingestion. Citrate- and PEG-CeO<sub>2</sub> (<10 nm) on the other hand appeared to translocate across the gut upon ingestion, as the clearance phase did not result in a significant loss of Ce and body burdens remained significantly greater in these worms than in non-exposed controls. Such translocation and cellular internalization of engineered nanomaterials in the gut has been observed in other aquatic worm species (García-Alonso et al. 2011). The OECD bioaccumulation test guideline TG315 recommends no gut clearance when sampling organisms during the uptake phase (OECD 2008) as this should return the most conservative bioaccumulation factors (BAF). However, this experiment demonstrates that careful consideration should be taken whether to measure and report body burdens that represent the concentration available for trophic transfer through food chains (feeding organisms including their gut contents) or that which remains accumulated within the organism after this material in the guts has been removed. This decision should perhaps be based (in part) on what the purpose of the accumulation study is, whether trying to seek understanding on what the possible capacity is for trophic transfer versus what the physiological effects imposed are on the exposed animal.

**Conclusions**

The environmental risk of engineered nanomaterials is a function of both hazard and exposure. This

study identifies differences in the route of uptake of nanoparticulate CeO<sub>2</sub> compared to its soluble counterpart Ce(III)NO<sub>3</sub> from contaminated sediments and provides explanation of this difference through assessment of the distribution of Ce during exposures between the solid bound, colloidal and dissolved LMW phases of the sediment. The additional route to uptake through transdermal accumulation of dissolved LMW species of a material has implications for partially soluble nanomaterials. It is currently unknown whether universal relationships between the route to uptake and the relative potential of a nanomaterial to elicit toxic effects in organisms can be established. As such, future work should address the mechanism by which dissolved species of partially soluble nanoparticles are accumulated in sediment biota and the potential for dietary and transdermal uptake of metal nanomaterials to induce different toxic effects. This will allow for a more nuanced understanding of the risk nanomaterials pose to sediment biota. Improved understanding of the fate processes which determine the route to uptake and the implications this may have for the toxicity of various engineered nanomaterials will also be valuable for incorporating safer-by-design strategies early in the development stage of new nano-enabled products. This study contributes to this effort, identifying different routes to uptake of nanoparticulate and dissolved LMW species of cerium from sediments in the aquatic worm *L. variegatus*.

### Disclosure statement

The authors report no conflicts of interest.

### Funding

This work was part of the GUIDEnano project by funding from the European Research Council under the European Union's Seventh Framework Programme grant №604387. The authors would also like to acknowledge the training and laboratory assistance provided by Dr Christine Elgy, FENAC (Facility for Environmental Nanoscience Analysis and Characterisation) under grant FENAC/2015/05/06. Tamara Galloway and Richard Cross also acknowledge financial support from Natural Environment Research Council (NERC NE/N006178). Also financial support was received from FP7 Nanosciences, Nanotechnologies, Materials and new Production Technologies.

### ORCID

Richard K. Cross  <http://orcid.org/0000-0001-5409-6552>

Tamara S. Galloway  <http://orcid.org/0000-0002-7466-6775>

### References

- Auffan, M., A. Masion, J. Labille, M.-A. Diot, W. Liu, L. Olivi, O. Proux, et al. 2014. "Long-Term Aging of a CeO<sub>2</sub> Based Nanocomposite Used for Wood Protection." *Environmental Pollution* 188:1–7. doi:10.1016/j.envpol.2014.01.016.
- Baker, T. J., C. R. Tyler, and T. S. Galloway. 2014. "Impacts of Metal and Metal Oxide Nanoparticles on Marine Organisms." *Environmental Pollution* 186:257–271. doi:10.1016/j.envpol.2013.11.014.
- Cornelis, G., J. K. Kirby, D. Beak, D. Chittleborough, and M. J. McLaughlin. 2010. "A Method for Determination of Retention of Silver and Cerium Oxide Manufactured Nanoparticles in Soils." *Environmental Chemistry* 7 (3): 298–308. doi:10.1071/EN10013.
- Cornelis, G., B. Ryan, M. J. McLaughlin, J. K. Kirby, D. Beak, and D. Chittleborough. 2011. "Solubility and Batch Retention of CeO<sub>2</sub> Nanoparticles in Soils." *Environmental Science & Technology* 45 (7):2777–2782. doi:10.1021/es103769k.
- Cornelis, G., C. DooletteMadeleine Thomas, M. J. McLaughlin, J. K. Kirby, D. G. Beak, and D. Chittleborough. 2012. "Retention and Dissolution of Engineered Silver Nanoparticles in Natural Soils." *Soil Science Society of America Journal* 76 (3):891. doi:10.2136/sssaj2011.0360.
- Cornelis, G., K. Hund-Rinke, T. Kuhlbusch, N. van den Brink, and C. Nickel. 2014. "Fate and Bioavailability of Engineered Nanoparticles in Soils: A Review." *Critical Reviews in Environmental Science and Technology* 44 (24): 2720–2764. doi:10.1080/10643389.2013.829767.
- Cross, R. K., C. Tyler, and T. S. Galloway. 2015. "Transformations That Affect Fate, Form and Bioavailability of Inorganic Nanoparticles in Aquatic Sediments." *Environmental Chemistry* 12 (6):627–642. doi:10.1071/EN14273.
- Dahle, J. T., K. Livi, and Y. Arai. 2015. "Effects of pH and Phosphate on CeO<sub>2</sub> Nanoparticle Dissolution." *Chemosphere* 119:1365–1371. doi:10.1016/j.chemosphere.2014.02.027.
- Dale, A. L., G. V. Lowry, and E. A. Casman. 2015. "Stream Dynamics and Chemical Transformations Control the Environmental Fate of Silver and Zinc Oxide Nanoparticles in a Watershed-Scale Model." *Environmental Science & Technology* 49 (12):7285–7293. doi:10.1021/acs.est.5b01205.
- Dogra, Y., K. P. Arkill, C. Elgy, B. Stolpe, J. Lead, E. Valsami-Jones, C. R. Tyler, et al. 2016. "Cerium Oxide Nanoparticles Induce Oxidative Stress in the Sediment-Dwelling Amphipod *Corophium volutator*." *Nanotoxicology* 10 (4):480–487. doi:10.3109/17435390.2015.1088587.
- Ferry, J. L., P. Craig, C. Hexel, P. Sisco, R. Frey, P. L. Pennington, M. H. Fulton, et al. 2009. "Transfer of Gold Nanoparticles from the Water Column to the Estuarine

- Food Web." *Nature Nanotechnology* 4 (7):441–444. doi:10.1038/nnano.2009.157.
- Galloway, T., C. Lewis, I. Dolciotti, B. D. Johnston, J. Moger, and F. Regoli. 2010. "Sublethal Toxicity of Nano-Titanium Dioxide and Carbon Nanotubes in a Sediment Dwelling Marine Polychaete." *Environmental Pollution* 158 (5): 1748–1755. doi:10.1016/j.envpol.2009.11.013.
- García-Alonso, J., F. R. Khan, S. K. Misra, M. Turmaine, B. D. Smith, P. S. Rainbow, S. N. Luoma, et al. 2011. "Cellular Internalization of Silver Nanoparticles in Gut Epithelia of the Estuarine Polychaete *Nereis Diversicolor*." *Environmental Science & Technology* 45 (10):4630–4636. pp. doi:10.1021/es2005122.
- Hammes, J. 2012. *Thesis: Evaluation of Sedimentation Rates of Engineered Nanoparticles in Natural Waters*. University of Trier. Germany.
- Hammes, J., J. A. Gallego-Urrea, and M. Hassellöv. 2013. "Geographically Distributed Classification of Surface Water Chemical Parameters Influencing Fate and Behavior of Nanoparticles and Colloid Facilitated Contaminant Transport." *Water Research* 47 (14):5350–5361. doi:10.1016/j.watres.2013.06.015.
- Heckert, E. G., S. Seal, and W. T. Self. 2008. "Fenton-Like Reaction Catalyzed by the Rare Earth Inner Transition Metal Cerium." *Environmental Science & Technology* 42 (13):5014–5019. doi:10.1021/es8001508.
- Hoppe, M., R. Mikutta, S. Kaufhold, J. Utermann, W. Duijnisveld, E. Wargenau, E. Fries., et al. 2016. "Retention of Sterically and Electrosterically Stabilized Silver Nanoparticles by Soil Minerals." *European Journal of Soil Science* 67 (5):573–582. doi:10.1111/ejss.12367.
- Karlsson, M. V., S. Marshall, T. Gouin, and A. B. A. Boxall. 2016. "Routes of Uptake of Diclofenac, Fluoxetine, and Triclosan into Sediment-Dwelling Worms." *Environmental Toxicology and Chemistry* 35 (4):836–842. doi:10.1002/etc.3020.
- Kettler, K., K. Veltman, D. van de Meent, A. van Wezel, and A. J. Hendriks. 2014. "Cellular Uptake of Nanoparticles as Determined by Particle Properties, Experimental Conditions, and Cell Type." *Environmental Toxicology and Chemistry* 33 (3):481–492. doi:10.1002/etc.2470.
- Labille, J., C. Harns, J.-Y. Bottero, and J. Brant. 2015. "Heteroaggregation of Titanium Dioxide Nanoparticles with Natural Clay Colloids." *Environmental Science & Technology* 49 (11):6608–6616. doi:10.1021/acs.est.5b00357.
- Leppänen, M. T., and J. V. K. Kukkonen. 1998. "Relative Importance of Ingested Sediment and Pore Water as Bioaccumulation Routes for Pyrene to Oligochaete (*Lumbricus variegatus*, Muller)." *Environmental Science & Technology* 32 (10):1503–1508. doi:10.1021/es970941k.
- Liu, X., G. Chen, and C. Su. 2012. "Influence of Collector Surface Composition and Water Chemistry on the Deposition of Cerium Dioxide Nanoparticles: QCM-D and Column Experiment Approaches." *Environmental Science & Technology* 46 (12):6681–6688. doi:10.1021/es300883q.
- Lohrer, A. M., S. F. Thrush, and M. M. Gibbs. 2004. "Bioturbators Enhance Ecosystem Function through Complex Biogeochemical Interactions." *Nature* 431 (7012): 1092–1095. doi:10.1038/nature03042.
- Lynch, I., 2016. "Water governance challenges presented by nanotechnologies: tracking, identifying and quantifying nanomaterials (the ultimate disparate source) in our waterways." *Hydrology Research* 47(3), 552–568. doi:10.2166/nh.2016.107
- Martinez, V. G., P. K. Reddy, and M. J. Zoran. 2006. "Asexual Reproduction and Segmental Regeneration, but Not Morphallaxis, Are Inhibited by Boric Acid in *Lumbricus variegatus* (Annelida: Clitellata: Lumbriculidae)." *Hydrobiologia* 564 (1):73–86. doi:10.1007/s10750-005-1709-9.
- Mount, D. R., T. D. Dawson, and L. P. Burkhard. 1999. "Implications of Gut Purging for Tissue Residues Determined in Bioaccumulation Testing of Sediment with *Lumbricus variegatus*." *Environmental Toxicology and Chemistry* 18 (6):1244–1249. doi:10.1002/etc.5620180625.
- Nam, D.-H., B.-C. Lee, I.-C. Eom, P. Kim, and M.-K. Yeo. 2014. "Uptake and Bioaccumulation of Titanium- and Silver-Nanoparticles in Aquatic Ecosystems." *Molecular & Cellular Toxicology* 10 (1):9–17. doi:10.1007/s13273-014-0002-2.
- O'Brien, N. J., and E. J. Cummins. 2011. "A Risk Assessment Framework for Assessing Metallic Nanomaterials of Environmental Concern: Aquatic Exposure and Behavior." *Risk Analysis* 31 (5):706–726. doi:10.1111/j.1539-6924.2010.01540.x.
- OECD 2008. *Test no. 315: bioaccumulation in sediment-dwelling benthic oligochaetes*. OECD. Accessed 2018-01-09.
- OECD 2012. *OECD Environment, Health and Safety Publications Series on the Safety of Manufactured Nanomaterials No 36. Guidance on Sample Preparation and Dosimetry for the Safety Testing of Manufactured Nanomaterials*. Organization for Economic Cooperation and Develop. Available at: [http://www.oecd.org/officialdocuments/publicdisplaydocumentpdf/?cote=ENV/JM/MONO\(2012\)40&docLanguage=En](http://www.oecd.org/officialdocuments/publicdisplaydocumentpdf/?cote=ENV/JM/MONO(2012)40&docLanguage=En) (Accessed: 9 January 2018).
- Prospect 2010. *Protocol for Nanoparticle Dispersion*. Available at: [http://www.nanotechia.org/sites/default/files/files/PROSPECT\\_Dispersion\\_Protocol.pdf](http://www.nanotechia.org/sites/default/files/files/PROSPECT_Dispersion_Protocol.pdf) (Accessed: 9 January 2018).
- Quik, J. T. K., M. C. Stuart, M. Wouterse, W. Peijnenburg, A. J. Hendriks, and D. van de Meent. 2012. "Natural Colloids Are the Dominant Factor in the Sedimentation of Nanoparticles." *Environmental Toxicology and Chemistry* 31 (5):1019–1022. doi:10.1002/etc.1783.
- Quik, J. T. K., D. van De Meent, and A. A. Koelmans. 2014. "Simplifying Modeling of Nanoparticle Aggregation-Sedimentation Behavior in Environmental Systems: A Theoretical Analysis." *Water Research* 62. 193–201. doi:10.1016/j.watres.2014.05.048.
- Rejman, J., V. Oberle, I. S. Zuhorn, and D. Hoekstra. 2004. "Size-Dependent Internalization of Particles via the Pathways of Clathrin- and Caveolae-Mediated Endocytosis." *Biochemical Journal* 377 (1):159–169. doi:10.1042/bj20031253.

- Roco, M. C., C. A. Mirkin, and M. C. Hersam. 2011. "Nanotechnology Research Directions for Societal Needs in 2020: summary of International Study." *Journal of Nanoparticle Research* 13 (3):897–919. doi:[10.1007/s11051-011-0275-5](https://doi.org/10.1007/s11051-011-0275-5).
- RStudio Team 2015. *RStudio: Integrated Development for R*. Boston: RStudio, Inc.
- Sang, W., et al. 2013. "Quantification of Colloid Retention and Release by Straining and Energy Minima in Variably Saturated Porous Media." *Environmental Science and Technology* 47 (15):8256–8264. doi:[10.1021/es400288c](https://doi.org/10.1021/es400288c).
- Simonin, M., and A. Richaume. 2015. "Impact of Engineered Nanoparticles on the Activity, Abundance, and Diversity of Soil Microbial Communities: A Review." *Environmental Science and Pollution Research* 22 (18):13710–13723. doi:[10.1007/s11356-015-4171-x](https://doi.org/10.1007/s11356-015-4171-x).
- Singh, C., et al. 2014. *Cerium Dioxide, NM-211, NM-212, NM-213: Characterisation and Test Item Preparation*. doi:[10.2788/80203](https://doi.org/10.2788/80203).
- Tombácz, E., and M. Szekeres. 2004. "Colloidal Behavior of Aqueous Montmorillonite Suspensions: The Specific Role of pH in the Presence of Indifferent Electrolytes." *Applied Clay Science* 27 (1–2):75–94. doi:[10.1016/j.clay.2004.01.001](https://doi.org/10.1016/j.clay.2004.01.001).
- Tourinho, P. S., C. A. M. van Gestel, S. Lofts, C. Svendsen, A. M. V. M. Soares, and S. Loureiro. 2012. "Metal-Based Nanoparticles in Soil: Fate, Behavior, and Effects on Soil Invertebrates." *Environmental Toxicology and Chemistry* 31 (8):1679–1692. doi:[10.1002/etc.1880](https://doi.org/10.1002/etc.1880).
- Vale, G., K. Mehennaoui, S. Cambier, G. Libralato, S. Jomini, and R. F. Domingos. 2016. "Manufactured Nanoparticles in the Aquatic Environment-Biochemical Responses on Freshwater Organisms: A Critical Overview." *Aquatic Toxicology* 170:162–174. doi:[10.1016/j.aquatox.2015.11.019](https://doi.org/10.1016/j.aquatox.2015.11.019).
- Whitley, A. R., C. Levard, E. Oostveen, P. M. Bertsch, C. J. Matocha, F. V D Kammer, J. M. Unrine., et al. 2013. "Behavior of Ag Nanoparticles in Soil: Effects of Particle Surface Coating, Aging and Sewage Sludge Amendment." *Environmental Pollution* 182:141–149. doi:[10.1016/j.envpol.2013.06.027](https://doi.org/10.1016/j.envpol.2013.06.027).
- Yang, G., Z. Sun, X. Lv, Y. Deng, Q. Zhou, and X. Huang. 2012. "Living Target of Ce(III) Action on Horseradish Cells: Proteins on/in Cell Membrane." *Biological Trace Element Research* 150 (1–3):396–402. doi:[10.1007/s12011-012-9514-6](https://doi.org/10.1007/s12011-012-9514-6).
- Yokel, R. A., et al. 2014. "The Yin: An Adverse Health Perspective of Nanoceria: uptake, Distribution, Accumulation, and Mechanisms of Its Toxicity." *Environmental Science: Nano* 1 (5):406–428. doi:[10.1039/C4EN00039K](https://doi.org/10.1039/C4EN00039K).
- Zhang, W., A. P. Schwab, J. C. White, and X. Ma. 2018. "Impact of Nanoparticle Surface Properties on the Attachment of Cerium Oxide Nanoparticles to Sand and Kaolin." *Journal of Environment Quality* 47 (1):129. doi:[10.2134/jeq2017.07.0284](https://doi.org/10.2134/jeq2017.07.0284).